

CuAgNPs-enzyme Biohybrids as Antimicrobial nanomaterials

Clara Ortega-Nieto,^a Noelia Losada-Garcia,^b Pilar Domingo-Calap,^c

Mirosława Pawlyta^d and Jose M. Palomo*^a

^aInstituto de Catálisis y Petroleoquímica (ICP). CSIC. 28049, Madrid, Spain

E-mail: josempalomo@icp.csic.es

^bInstitute for Integrative Systems Biology (I²SysBio). Universitat de València-CSIC

46980, Paterna, Spain

^cMaterials Research Laboratory, Faculty of Mechanical Engineering, Silesian University of

Technology, Konarskiego 18A, 44-100, Gliwice, Poland

Abstract

Multidrug-resistant bacterial infections have become major threats to public health worldwide. Thus, bimetallic Ag-Cu nanoparticles-enzyme biohybrids has been developed. Different bimetallic bionanohybrids were synthesized with different contents of Ag, by the direct incubation of a previously synthesized $\text{Cu}_3(\text{PO}_4)_2$ NPs-CALB hybrid with silver salt in aqueous media and r.t. They were fully characterized, determining silver phosphate as metal species, and different nanoparticles sizes depending on the amount of silver used. HAADF-STEM analyses demonstrated the formation of individual Ag_3PO_4 NPs on the Cu-CALB nanoflowers. The catalytic reductase or oxidase-like activities of the bimetallic biohybrids was also affected being higher values when lower amount of silver was used. This effect was corroborated in their antimicrobial efficacy against *Escherichia coli*, *Klebsiella pneumoniae*, *Pseudomonas aeruginosa* and *Mycobacterium smegmatis*. Results indicate that the presence of small content on silver in the bimetallic hybrids highly enhanced the antibacterial activity compared to initial Cu_{36} @CALB hybrid. Optimal amount of silver has been found corresponding to the bimetallic $\text{Ag}_4\text{Cu}_{32}$ @CALB hybrid which showed the strongest antibacterial effect, with log reductions of 7.6, 4.3 and 3.9 for *K. pneumoniae*, *P. aeruginosa*, *E. coli*, and 1.8 for *M. smegmatis*. Overall, these novel nanomaterials are a promising alternative for fight against different pathogens.

Keywords: silver phosphate, copper phosphate, nanoparticles, biohybrids, antimicrobial activity, multi-drug resistant bacteria

Introduction

Antimicrobial resistance has become a significant global health concern in recent times. According to recent studies, superbugs are responsible for over 4.95 million deaths annually.^{1,2} As bacteria evolve and develop resistance to traditional antibiotics, new and innovative approaches need to be explored to combat this growing crisis.

One promising avenue is the use of nanomaterials in the fight against antibacterial resistance. Nanomaterials, characterized by their unique physical and chemical properties at the nanoscale, exhibit properties such as increased surface area, improved drug delivery and unique interactions with bacterial cells and have shown great potential in enhancing the effectiveness of antibacterial treatments.^{3,4}

In particular, metal nanoparticles have emerged as promising candidates for antibacterial agents due to their unique properties and versatile applications. Several metals, such as silver or copper, have demonstrated notable antibacterial effects, opening new avenues for combating microbial infections.⁵⁻⁹ In addition, combinations of various metals in nanomaterials present numerous advantages compared to nanoparticles consisting of a single metal. These advantages include improved properties, leading to synergistic effects and customized features, multifunctionality, stability, cost-effectiveness, and the potential for novel applications.¹⁰⁻¹³

Indeed, bimetallic nanoparticles have been able to inhibit bacterial growth through the following mechanisms: i) Adhesion to the cell membrane altering its structure, permeability and deficiencies in cell functions such as ATP secretion and transport activity. ii) Penetration into the cell and nucleus by disrupting mitochondrial function, destabilise and denature proteins, ribosomes and DNA interaction. iii) Oxidase like-activity by generating reactive oxygen species (ROS) that can oxidise proteins, lipids and DNA bases.^{12,13}

However, the synthesis of metal nanostructures could represent an important challenge. In this way, we have used a pioneer method where an enzyme is used in the *in situ* formation of the

nanoparticles. In this strategy, the enzyme plays key roles because apart of being the inductor of the metal nanoparticle formation, serves as a stabilizing agent, allowing to produce homogeneously dispersed nanoparticles embedded in the protein matrix network. This method allows to obtain heterogeneous materials, the so called metal-enzyme nanobiohybrids, in aqueous media at room temperature and without using external agents. Also this methodology, because of the protein structure per se, it is able to control the growth of the nanoparticle even affecting the morphology, which is directly related to the improvement in their catalytic activity as nanozymes.¹⁴⁻¹⁶

Thus, in the present work we have developed novel bimetallic copper-silver-enzyme systems, based on the AgNPs-formation directly induced by the enzyme using as scaffold a previous Cu bionanohybrid, created using *C. antarctica* B lipase and copper salt to form $\text{Cu}_3(\text{PO}_4)_2\text{NPs}$ -CALB hybrid (**Figure 1**).¹⁷⁻²⁰ The incorporation of different concentrations of silver in the generation of the new bimetallic hybrids will be evaluated, where the formation of the different metal species, the metal content and the effect on the formation of nanoparticles, as well as their catalytic enzyme-like activity will be assessed.

This $\text{Cu}_{36}\text{@CALB}$ bionanohybrid exhibited excellent antiviral and catalytic performance in previous studies.¹⁷⁻¹⁸ However, its antibacterial activity was not as pronounced as its antiviral one. With the addition of as a second metal, we expected to improve the antibacterial activity of the hybrid system. The addition of silver as a secondary metal was thought as suitable for the objective, thanks to its recognized antibacterial properties.²¹

Furthermore, the combination of two metals could produce synergistic effects that enhance the activity of bionanohybrids.^{8,10,13}

To evaluate their antibacterial effectiveness, the Cu-Ag bionanohybrids were confronted to several bacterial strains, including *Escherichia coli*, *Klebsiella pneumoniae* and *Pseudomonas aeruginosa*. These strains were chosen because they are among the top six pathogens

responsible for the most deaths due to antimicrobial resistance, according to the literature.^[2] In addition, they were tested against the gram-positive bacteria *Mycobacterium smegmatis*.

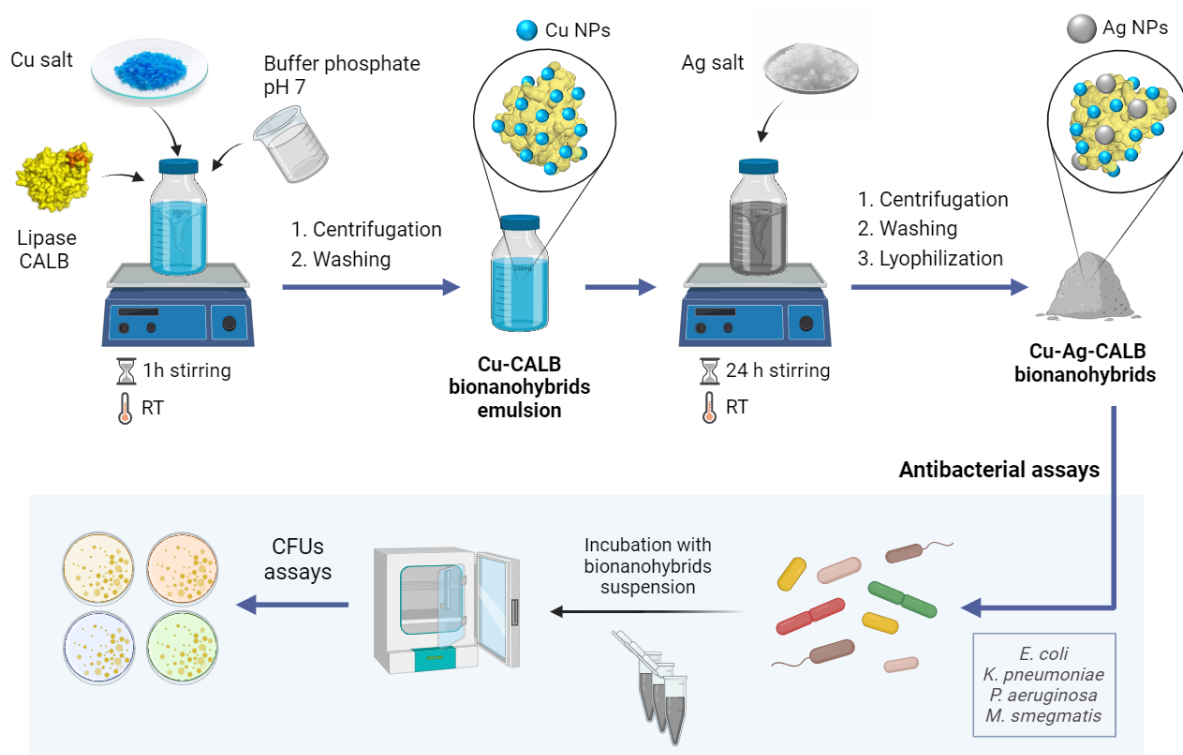


Figure 1. Illustrative scheme of the synthesis and antimicrobial evaluation of Ag-Cu bionanohybrids.

Results and discussion

Synthesis and Characterization of Ag-Cu nanoparticles-enzyme biohybrids

The silver-copper-CALB hybrids were synthesized from a previously developed $\text{Cu}_3(\text{PO}_4)_2\text{NPs}$ -CALB bionanohybrid,^{17,18} which contained 36 wt% of Cu ($\text{Cu}_{36}\text{@CALB}$ hybrid). In this way, different amounts of silver nitrate per mL of Cu hybrid were added to aqueous solution of $\text{Cu}_{36}\text{@CALB}$ hybrid and the mixture was incubated for 24 h at r.t. in magnetic stirring and after that the mixture was centrifuged and the solid obtained was washed and lyophilized to get eight different nanobiohybrids. After ICP-OES analyses, the weight-by-weight percentage of copper and silver content in each hybrid was determined, as shown in **Table 1**.

The maximum amount of silver added was established according to data from our previous research, where the maximum concentration of silver required to create a Ag-CALB hybrid was defined as 60 mg of Ag salt per mg of enzyme.²² Following this premise and knowing that the Cu hybrid emulsion (in aqueous media) has a concentration of 5000 ppm, 12 mg of silver salt per mL of $\text{Cu}_{36}\text{@CALB}$ was determined to create the Ag-Cu bimetallic hybrid with the maximum (100%) amount of silver, which was called as $\text{Ag}_{32}\text{Cu}_8\text{@CALB}$ (Table 1). Afterwards, in search of the most effective antimicrobial bimetallic hybrid with the less quantity of silver in its composition, the silver salt concentration was reduced to 6, 3, 1.2, 0.6, 0.36, 0.24 and 0.12 mg per mL of $\text{Cu}_{36}\text{@CALB}$, obtaining hybrids with different content of silver (measured by ICP-OES) from 15 to 1 wt%, the so-called hybrids $\text{Ag}_{15}\text{Cu}_{21}\text{@CALB}$, $\text{Ag}_8\text{Cu}_{28}\text{@CALB}$, $\text{Ag}_6\text{Cu}_{30}\text{@CALB}$, $\text{Ag}_4\text{Cu}_{32}\text{@CALB}$, $\text{Ag}_2\text{Cu}_{34}\text{@CALB}$, $\text{Ag}_{1.5}\text{Cu}_{35}\text{@CALB}$ and $\text{Ag}_1\text{Cu}_{35}\text{@CALB}$, respectively (Table 1).

In addition, the amount of copper in the bionanohybrid decreased as more silver was added. This indicates that when silver enters the Cu hybrid, copper leaves the structure. When the maximum amount of silver nitrate was added in $\text{Ag}_{32}\text{Cu}_8\text{@CALB}$ hybrid, silver percentage was 32wt%, instead of 8wt% of Cu remaining of the total metal content.

Table 1. Ag-Cu bionanohybrids synthesis details and weight percentage of silver and copper.

Bionanohybrid	Ag added to Cu hybrid [wt%]	Ag amount ^a	Ag [wt%] ^b	Cu [wt%] ^b
Ag ₃₂ Cu ₈ @CALB	100%	12	31.7%	7.6%
Ag ₁₅ Cu ₂₁ @CALB	50%	6	15.0%	21.3%
Ag ₈ Cu ₂₈ @CALB	25%	3	8.1%	28.3%
Ag ₆ Cu ₃₀ @CALB	10%	1.2	6.1%	30.5%
Ag ₄ Cu ₃₂ @CALB	5%	0.6	3.7%	32.3%
Ag ₂ Cu ₃₄ @CALB	3%	0.36	2.0%	34.1%
Ag _{1.5} Cu ₃₅ @CALB	2%	0.24	1.5%	34.7%
Ag ₁ Cu ₃₅ @CALB	1%	0.12	0.9%	35.4%
Cu ₃₆ @CALB	0%	0	0.0%	36.0%

^a amount in mg of silver nitrate added to each mL of Cu-CALB hybrid solution (5 g/L). ^b metal content in each mg of solid determined by ICP-OES analysis.

In this case the copper content was reduced in 78% compared to the original Cu₃₆@CALB hybrid. When the addition of silver was 50%, the amount of Cu exchanged by Ag in this hybrid was of 15wt% (Ag₁₅Cu₂₁@CALB hybrid). This trend was observed in the rest of the hybrids, being more proportional in term of the amount of Cu exchange, at lower quantities of silver used (Table 1).

Only at 100% silver nitrate amount, higher metal percentage was achieved. Indeed, the XRD analysis of Ag₃₂Cu₈@CALB hybrid showed the formation of silver phosphate as metal species by an almost 90% exchange of Cu²⁺ by Ag⁺ (**Figure S1**). The diffraction peaks (110), (200), (210), (211), (220), (310), (320), (321) and (400) correlated perfectly with the Ag₃PO₄ standard data (JCPDS card no. 06-0505).²³ This phenomenon could be explained by the highest affinity of Ag⁺ ions against phosphate groups (PO₄³⁻) compared to Cu²⁺. Furthermore, it has been described some examples in copper metalloproteins, where Ag⁺ might be able to compete with

the endogenous copper, when the active site bound to the cupric form is positioned in a solvent-exposed medium, existing the $\text{Ag} \rightarrow \text{Cu}$ substitution, by releasing the Cu^{2+} into the surrounding medium.^{24,25} In these hybrids the enzyme plays a key role as scaffold also involved in the metal coordination which also can be considered in the metal exchange process.

In the XRD analyses of $\text{Ag}_{15}\text{Cu}_{21}@CALB$, the silver phosphate peaks can be easily appreciated (Figure 2), but with lower intensities than in $\text{Ag}_{32}\text{Cu}_8@CALB$. Additional peaks that match well with the Cu_3PO_4 standard (JCPDS card no. 022-0548) have been observed. The same trend was observed in $\text{Ag}_8\text{Cu}_{28}@CALB$, where it can be seen how the peaks corresponding to Cu_3PO_4 become more predominant compared to those of Ag_3PO_4 (Figure 2).

Thus, as the silver content decreased in $\text{Ag}_6\text{Cu}_{30}@CALB$, $\text{Ag}_4\text{Cu}_{32}@CALB$, $\text{Ag}_2\text{Cu}_{34}@CALB$, $\text{Ag}_{1.5}\text{Cu}_{35}@CALB$ and $\text{Ag}_1\text{Cu}_{35}@CALB$, the silver phosphate peaks, particularly (200), (210) or (211), in XRD analyses disappeared, being X-ray diffraction pattern more similar to the original. X-ray photoelectron spectroscopy (XPS) confirmed the presence of Ag(I) and Cu(II) as metal species, for example in $\text{Ag}_4\text{Cu}_{32}@CALB$ hybrid (**Figure S2**)

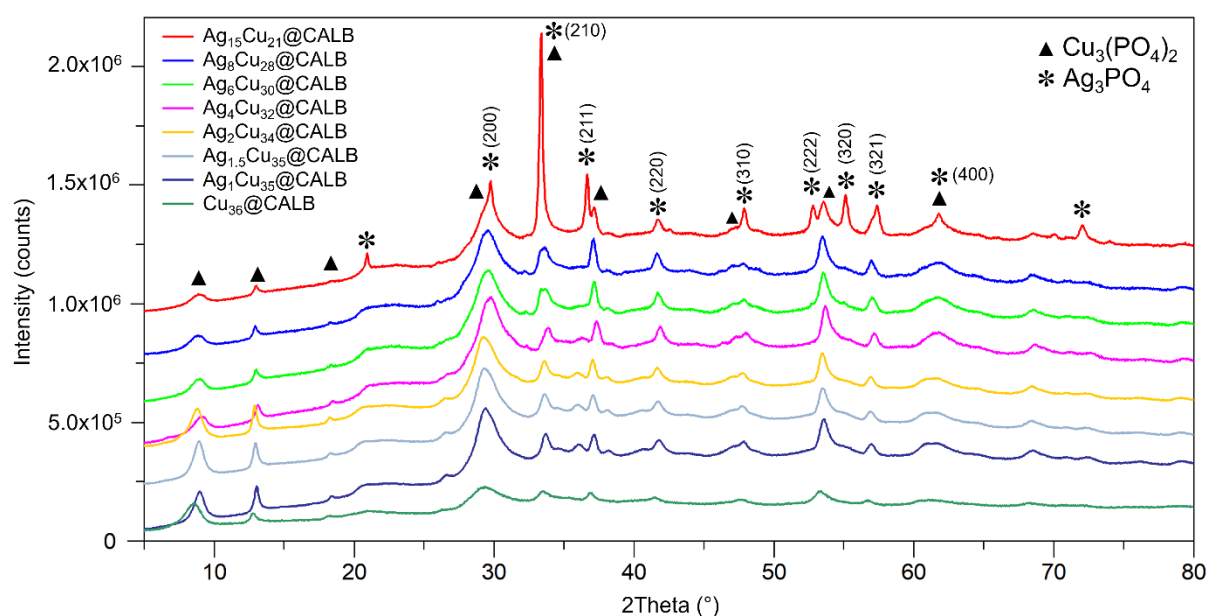


Figure 2. XRD spectra of Ag-Cu bionanohybrids.

TEM and STEM characterization demonstrated the presence of nanocrystals with lengths greater than 200 nm and spherical crystalline nanoparticles between 2 and 44 nm in Ag₃₂Cu₈@CALB (Figure S3). TEM analyses of the rest of the hybrids also revealed the formation of spherical nanoparticles, with different diameter sizes ranging from 1.6 to 27.1 nm (**Figure 3, Figures S4-S10**), which are distributed on the surface of the nanostructure. It is important to note that the synthesis of the silver-copper hybrids begins with a nanoflower structure comprising copper nanoparticles with an average size of 4 nm (Cu₃₆@CALB).

The larger particles sizes were observed in Ag₃₂Cu₈@CALB, Ag₁₅Cu₂₁@CALB and Ag₈Cu₂₈@CALB, where supramolecular more aggregated structures were obtained (Figures 3 a-b, Figure S3), where it was able to found nanoparticles with 44 nm diameter size in the case of Ag₃₂Cu₈@CALB (Figure S3), whereas bimetallic biohybrids with lower content in silver, Ag₃₂Cu₈@CALB, Ag₁₅Cu₂₁@CALB presented nanoparticles with diameter from 10 to 24 nm (Figures 3a,b). The reduction in the content in silver (w/w) during the synthesis, generated biohybrids with more dispersed nanoflower structures, although still some larger nanoparticle could be found but mainly lower than 20 nm (Figures 3 c-g). In Ag₆Cu₃₀@CALB, and Ag₄Cu₃₂@CALB the presence of nanorods structure were observed in TEM (Figure 3c-d).

Only in the 1% (w/w) silver content biohybrid (Ag₁Cu₃₅@CALB) was able to find nanoparticles with diameter larger near 10 nm (Figure 3g). However, mostly in general the diameter average size of nanoparticles in the different bio-hybrids were lower than 8 nm, being the highest at 6.3 nm for Ag₃₂Cu₈@CALB, decreasing the particle size when amount of silver decreased, between 5-5.7 nm for Ag₁₅Cu₂₁@CALB and Ag₈Cu₂₈@CALB. This average size decrease to 4.1-4.5 in the case of Ag₆Cu₃₀@CALB, Ag₄Cu₃₂@CALB and Ag₂Cu₃₄@CALB and it was around 4 nm or lower in Ag_{1.5}Cu₃₅@CALB and Ag₁Cu₃₅@CALB the NPs, respectively (Figure 3).

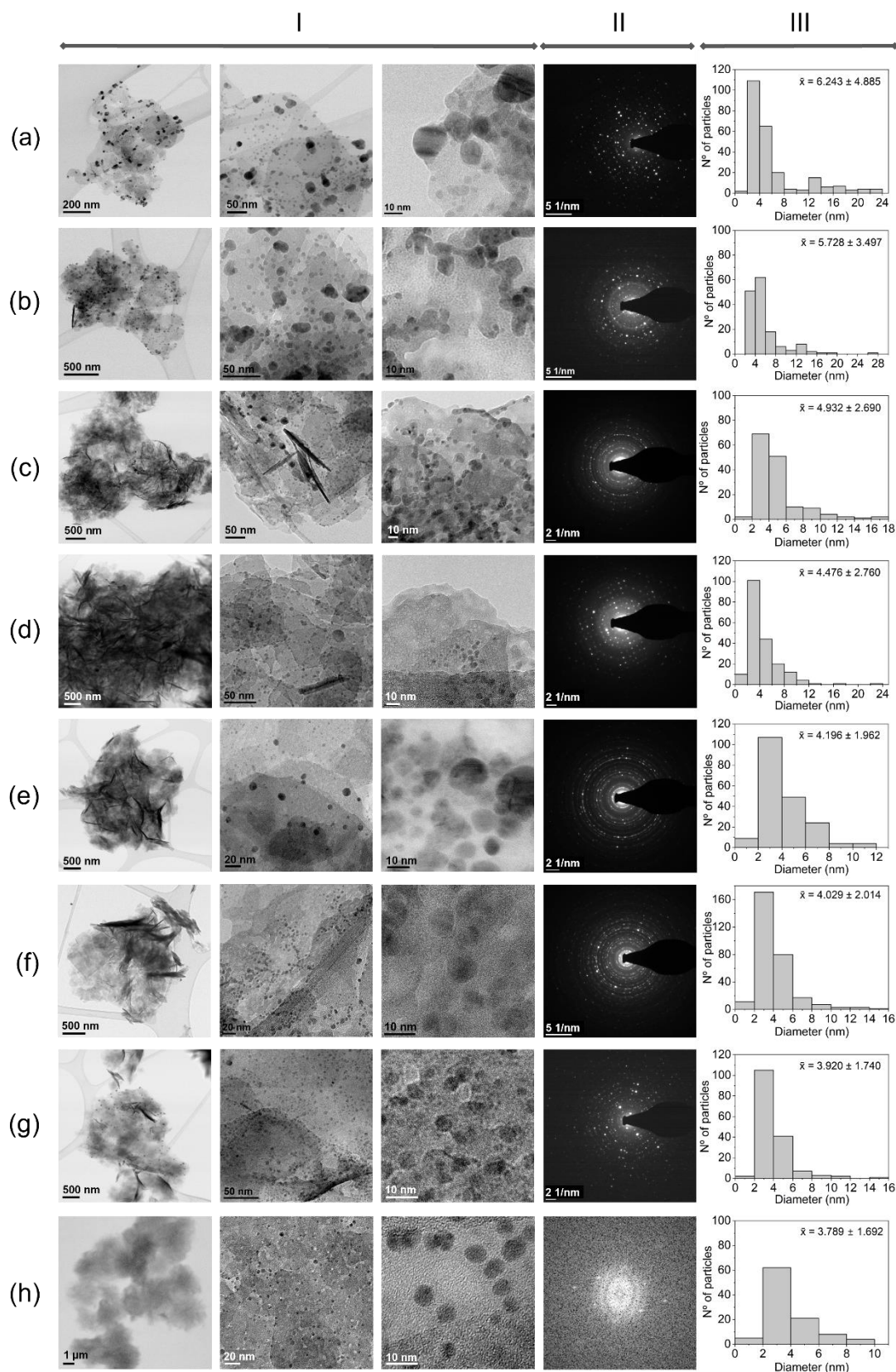


Figure 3. Characterization of Cu-Ag bionanohybrids: a) Ag₁₅Cu₂₁@CALB, b) Ag₈Cu₂₈@CALB, c) Ag₆Cu₃₀@CALB, d) Ag₄Cu₃₂@CALB, e) Ag₂Cu₃₄@CALB, f) Ag_{1.5}Cu₃₅@CALB, g) Ag₁Cu₃₅@CALB and h) Cu₃₆@CALB. (I) TEM and HRTEM images; (II) FT and (III) NPs size distribution.

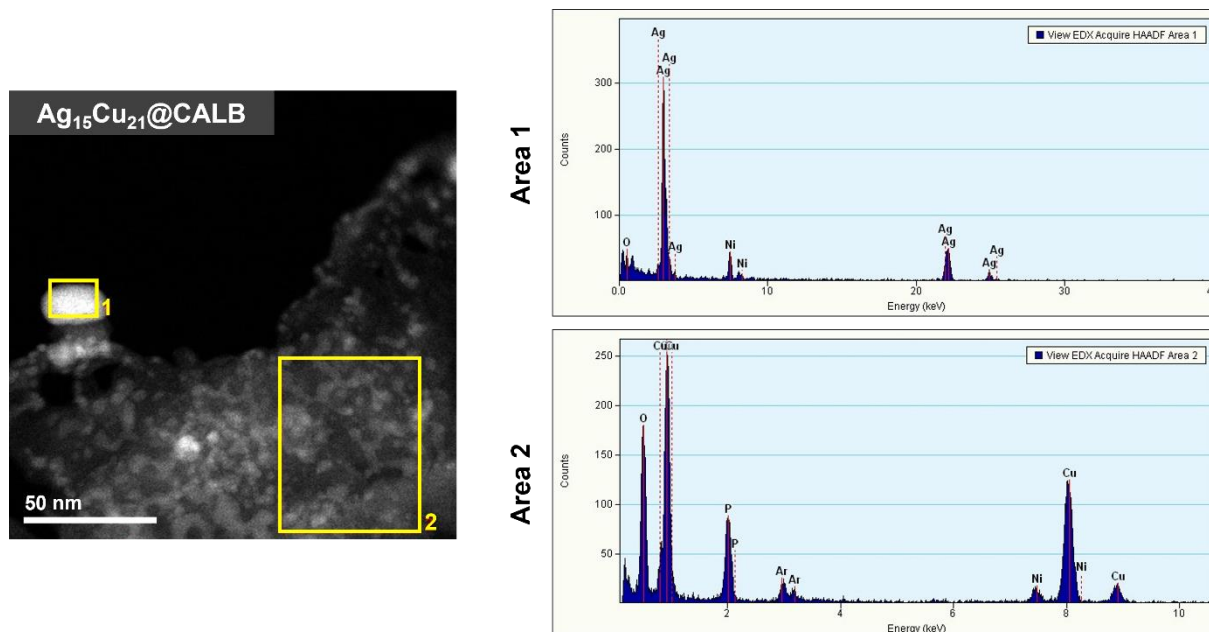


Figure 4. HAADF-STEM-EDX characterization of $\text{Ag}_{15}\text{Cu}_{21}\text{@CALB}$ hybrid. The nickel signal corresponds to the grid used for the experiment.

Then, to figure out the structural composition of the NPs and their localization, HAADF-STEM images and EDX maps were performed.

In $\text{Ag}_{32}\text{Cu}_8\text{@CALB}$, results determined that the nanocrystals previously described were mainly made of silver phosphate, and oxygen, and this, together with the previous XRD results, suggests that these are silver phosphate crystals (**Figure S11**).

HAADF-STEM-EDX characterization of $\text{Ag}_{15}\text{Cu}_{21}\text{@CALB}$ showed that larger particles corresponded to AgNPs were located on the surface of the nanoflowers, containing very small nanoparticles of copper phosphate (**Figure 4**). Similar results were observed for the rest of the hybrids as well (**Figures S12-S17**). Also, it can be observed that the metal NPs with diameter average size between 6 and 24 nm were silver nanoparticles, while the NPs with about 4 nm were composed of copper.

Catalytic Activity Evaluation

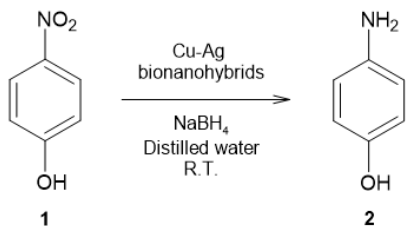
Evaluation of reductase-like activity of the different Ag/Cu-hybrids

The catalytic activity of the biohybrids nanozymes was tested in the reduction of *p*-nitrophenol (pNP) to *p*-aminophenol (pAP), in water at room temperature. In a previous research, we observed that the precursor copper hybrid (Cu₃₆@CALB) did not show any reductase-like activity in this reaction when employing 2mL of pNP 1mM. Therefore, it was used to evaluate the effect of silver incorporation in the final activity of the new Ag-Cu bionanohybrids. Surprisingly, the Ag-Cu hybrids were ultrafast under these conditions (data not shown). Then, these bimetallic hybrids were evaluated as catalysts using 50 times higher pNP concentration (50mM) (Table 2).

The highest efficiency was found for the hybrid with less silver amount, Ag₁Cu₃₅@CALB, with a TOF value of 397.5 min⁻¹. Also, it can be appreciated how TOF values decreased as the amount of silver in the hybrid increases, so the lowest value was obtained for Ag₃₂Cu₈@CALB hybrid (49.1 min⁻¹).

These results could be explained considering the nanostructures formed in the different hybrids. At higher concentration of silver, AgNPs are more in aggregated formed and larger, whereas lower content of silver allowed to obtain homogeneous distributed smaller AgNPs on Cu-nanoflower surface, making more active sites accessible and higher superficial area.

Thus, bimetallic nanozyme containing very low amount of silver (Ag₁Cu₃₅@CALB hybrid) caused a huge reductase-like activity enhancement (up to almost 400 times) compared to the original copper hybrid. Moreover, if we compare these results with the data obtained for a CALB hybrid with only Ag in its composition,²² a clear improvement can be also observed.

Table 2. Hydrogenation of *p*-nitrophenol catalyzed by Ag-Cu bionanohybrids ^{a)}

Hybrid	Time [min]	Hybrid amount [mg]	Ag in the hybrid [wt%]	pNP conversion [%]	TOF ^{b)} [min ⁻¹]
Ag ₃₂ Cu ₈ @CALB	0.5	1	31.7%	72.0%	49.1
Ag ₁₅ Cu ₂₁ @CALB	0.5	1	15.0%	39.3%	56.7
Ag ₈ Cu ₂₈ @CALB	0.5	1	8.1%	41.9%	112.1
Ag ₆ Cu ₃₀ @CALB	0.5	1	6.1%	41.4%	146.8
Ag ₄ Cu ₃₂ @CALB	0.5	1	3.7%	48.6%	284.8
Ag ₂ Cu ₃₄ @CALB	1	1	2.0%	40.4%	217.1
Ag _{1.5} Cu ₃₅ @CALB	1	1	1.5%	29.8%	221.3
Ag ₁ Cu ₃₅ @CALB	1	1	0.9%	33.9%	397.5

^{a)} Conditions: 50 mM **1**, 2 M NaBH₄, 2 mL distilled water, R.T.; ^{b)} TOF value was defined as the converted moles of **1** per moles of silver metal atoms in the bionanohybrid per minute.

Evaluation of oxidase like-activity of the different Ag/Cu-hybrids

The oxidative capacity of the nanozyme hybrids was also tested in the oxidation of *p*-aminophenol (pAP) in water at room temperature (Table 3). This reaction represents a mimetic indirect assay of the ROS capacity of the nanozymes (Fenton-type reaction), which have been recently successfully used to corroborate antiviral activity of different nanozymes.¹⁷⁻¹⁸

In this case the precursor Cu₃₆@CALB hybrid showed good activity against the oxidation of pAP to benzoquinone with 50% conversion in 5 min (Table S1). The incorporation of Ag in the bimetallic nanohybrid clearly demonstrate that Ag phosphate also showed Fenton capacity even higher than Cu phosphate at these conditions. Considering the silver content in the hybrid, the highest TOF value was achieved when amount of silver was lower in the bimetallic nanozyme

(Table 3), obtaining 2 times higher values for Ag₄Cu₃₂@CALB against Ag₃₂Cu₈@CALB and more than 5 times higher for Ag₁Cu₃₅@CALB. Evaluating the amount of copper, the best TOF value was achieved by Ag₃₂Cu₈@CALB, whereas for the rest of catalysts this value was quite similar to that achieved for Cu₃₆@CALB. Thus, these results showed that, considering same total content metal from only copper or bimetallic hybrids, the latter showed higher performance in term of conversion.

Table 3. Oxidation of *p*-aminophenol catalyzed by Ag-Cu bionanohybrids ^{a)}

Hybrid	Time [min]	Hybrid amount [mg]	Ag in the hybrid [wt%]	pAP conversion [%]	TOF ^{b)} [min ⁻¹]
Ag ₃₂ Cu ₈ @CALB	2	3	31.7%	77.4%	0.44
Ag ₁₅ Cu ₂₁ @CALB	5	3	15.0%	72.3%	0.35
Ag ₈ Cu ₂₈ @CALB	5	3	8.1%	32.3%	0.29
Ag ₆ Cu ₃₀ @CALB	5	3	6.1%	22.5%	0.27
Ag ₄ Cu ₃₂ @CALB	5	3	3.7%	51.8%	1.01
Ag ₂ Cu ₃₄ @CALB	5	3	2.0%	49.1%	1.76
Ag _{1.5} Cu ₃₅ @CALB	5	3	1.5%	55.8%	2.77
Ag ₁ Cu ₃₅ @CALB	5	3	0.9%	36.3%	2.84

^{a)} Conditions: 1 mM pAP, 50 mM H₂O₂, 10 mL distilled water, R.T.; ^{b)} TOF value was defined as the converted moles of 1 per moles of silver metal atoms in the bionanohybrid per minute.

Antibacterial Assays

In a first step, the antimicrobial activity of the developed hybrids was tested in a concentration of 125 ppm against *Escherichia coli* after a 4-hours incubation. **Figure 5** shows that the hybrids Ag₆Cu₃₀@CALB and Ag₄Cu₃₂@CALB, with a modest amount of silver, achieved 4.0 and 3.9

\log_{10} bacterial reduction. $\text{Ag}_{32}\text{Cu}_8@\text{CALB}$, $\text{Ag}_{15}\text{Cu}_{21}@\text{CALB}$ and $\text{Ag}_8\text{Cu}_{28}@\text{CALB}$ hybrids, with much more silver in their composition, resulted in a 34% lower efficiency.

This showed the improvement of antibacterial activity against *E. coli* by bimetallic hybrids compared to $\text{Cu}_{36}@\text{CALB}$. However, when amount of silver was less than 3%, $\text{Ag}_2\text{Cu}_{34}@\text{CALB}$, $\text{Ag}_{1.5}\text{Cu}_{35}@\text{CALB}$ or $\text{Ag}_1\text{Cu}_{35}@\text{CALB}$ bionanohybrids, antibacterial effect was drastically reduced, reaching similar values to those of $\text{Cu}_{36}@\text{CALB}$ in the conditions described (Figure 5).

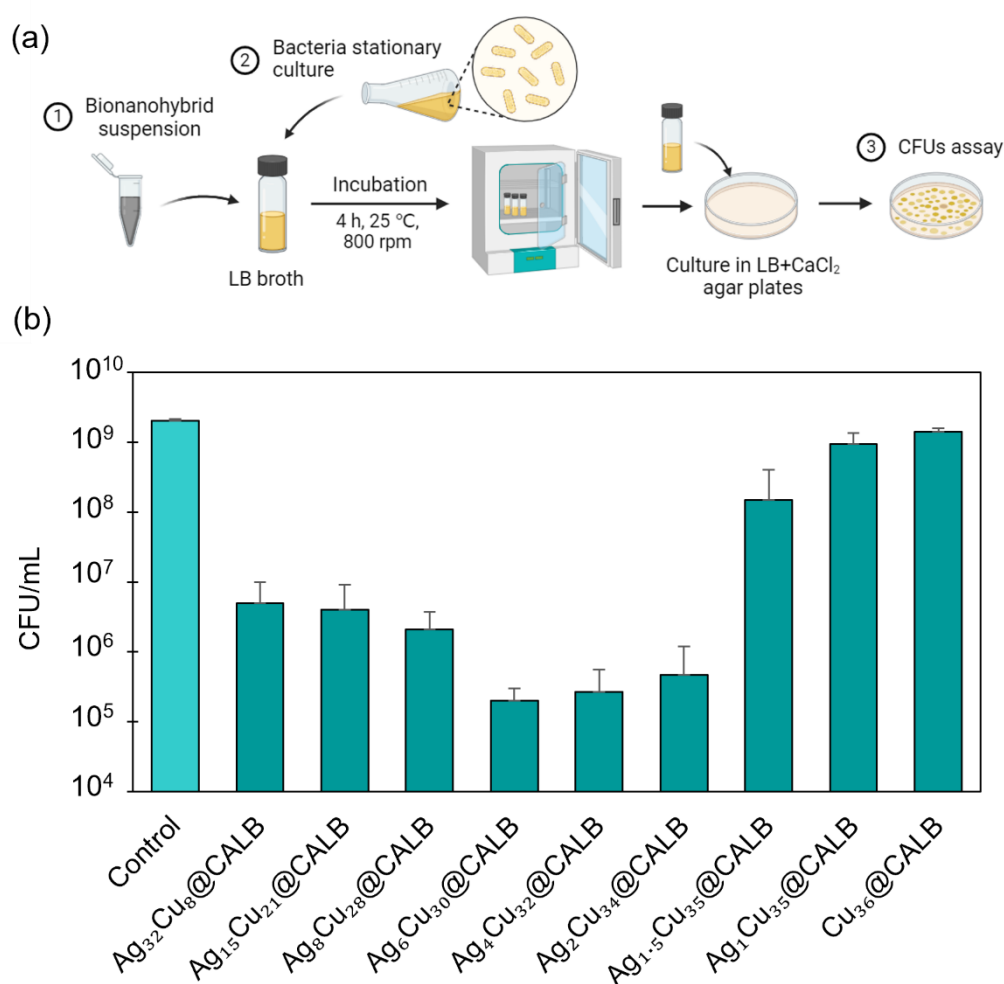


Figure 5. a) Illustrative scheme of the method. b) Antibacterial effect of Ag-Cu bionanohybrids in a concentration of 125 ppm against *E. coli* after a 4h incubation. Graph shows the average of three different assays in CFU/mL. Error bars correspond to standard deviation.

This phenomenon occurs in hybrids with an amount of silver below 3%, which may suggest that the silver particles, being in such a low quantity, are not sufficiently available to exert the antibacterial effect previously observed. Conversely, several studies have indicated that the size of the silver NPs is not a constant factor influencing the antibacterial effect, but that other crucial factors come into play, such as the release of ions, the surface charge, or the capacity to generate ROS.²⁶⁻²⁸

To further investigate this hypothesis, the bionanohybrids with less amount of silver ($\text{Ag}_4\text{Cu}_{32}@CALB$, $\text{Ag}_2\text{Cu}_{34}@CALB$, $\text{Ag}_{1.5}\text{Cu}_{35}@CALB$ and $\text{Ag}_1\text{Cu}_{35}@CALB$) were selected for extra experiments with two gram-negative bacteria of current health concern: *Klebsiella pneumoniae*, *Pseudomonas aeruginosa*; and a gram-positive mycobacterium, *Mycobacterium smegmatis*. The different strains were incubated with the hybrids for 4 hours with a 1000 ppm hybrid concentration. Results are presented in **Figure 6 (a-c)**.

With *K. pneumoniae*, the inhibition profile was comparable to that of *E. coli*, with high inhibition values observed for $\text{Ag}_4\text{Cu}_{32}@CALB$ and $\text{Ag}_2\text{Cu}_{34}@CALB$, at 7.8 and 6.6 log reduction, respectively. The efficacy of $\text{Ag}_{1.5}\text{Cu}_{35}@CALB$ was 50%, while that of $\text{Ag}_1\text{Cu}_{35}@CALB$ was practically inactive.

In the case of *P. aeruginosa*, the differences between $\text{Ag}_4\text{Cu}_{32}@CALB$, $\text{Ag}_2\text{Cu}_{34}@CALB$ and $\text{Ag}_{1.5}\text{Cu}_{35}@CALB$ were not significant, reaching high log reduction values in all cases, approaching to 4 log₁₀. $\text{Ag}_1\text{Cu}_{35}@CALB$, as previously observed, did not demonstrate any antibacterial capacity.

The antibacterial effect against *M. smegmatis* was markedly inferior with respect to the rest of the bacteria. Even so, $\text{Ag}_4\text{Cu}_{32}@CALB$ achieved an 89.2% of inhibition. However, no significant antibacterial effect against *M. smegmatis* was observed with hybrids $\text{Ag}_2\text{Cu}_{34}@CALB$, $\text{Ag}_{1.5}\text{Cu}_{35}@CALB$ and $\text{Ag}_1\text{Cu}_{35}@CALB$. This can be explained by the

gram-positive nature of *M. smegmatis*, distinguishing it from the others, gram-negative. Their peptidoglycan layer makes it more resistant to bionanohybrids attack than gram-negative bacteria, which have a thinner peptidoglycan layer and an outer layer composed of lipopolysaccharides, lipoproteins, and lipids.²⁹

To determine if a longer exposure of the hybrids to *M. smegmatis* would have a greater effect, a second experiment was conducted for 16 hours while maintaining the 1000 ppm hybrids concentration. The results of the experiment revealed an improvement in the antibacterial effect of all the hybrids (Figure 6d). The Ag₄Cu₃₂@CALB hybrid demonstrated the highest activity, achieving a 98.5% inhibition rate, while Ag₂Cu₃₄@CALB, Ag_{1.5}Cu₃₅@CALB and Ag₁Cu₃₅@CALB obtained inhibition rates of 95.2%, 77.3% and 76.6%, respectively.

On the other hand, it was aimed to test whether a reduction in the concentration of the hybrids against *K. pneumoniae* had any impact on their effectiveness. For this purpose, Ag₄Cu₃₂@CALB and Ag₂Cu₃₄@CALB were selected, as being the best hybrids against *K. pneumoniae* in the 1000 ppm experiment. The concentration of the hybrids was set to 200 ppm and the exposure time to 4 hours. Ag₄Cu₃₂@CALB exhibited superior antibacterial efficacy compared to Ag₂Cu₃₄@CALB, with log reductions of 3.5 and 1.2, respectively (Figure 6e). Although still significant, the values were lower with respect to the 1000 ppm test, which indicates that the concentration of the hybrids is dependent on their antibacterial power.

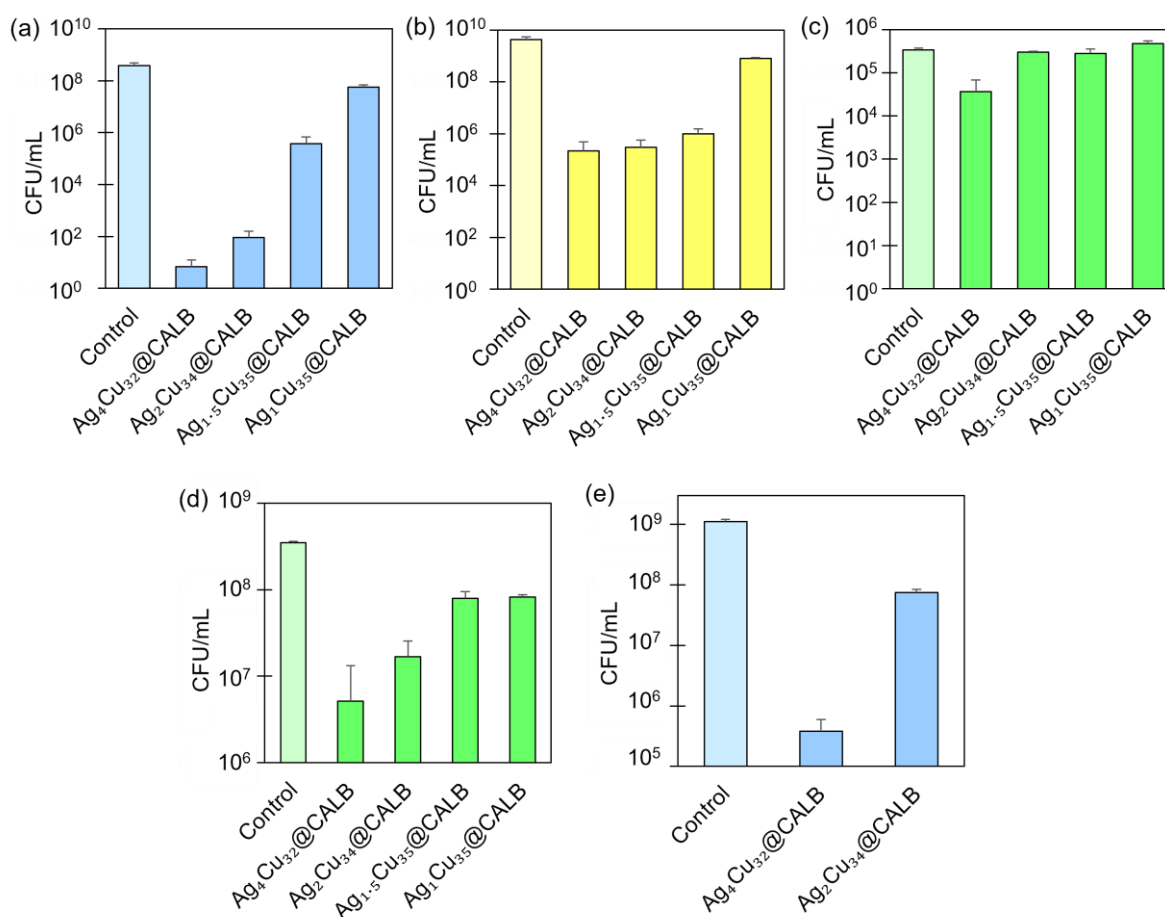


Figure 6. Antibacterial effect of Ag-Cu bionanohybrids in a concentration of 1000 ppm after a 4h incubation against: a) *Klebsiella pneumoniae*, b) *Pseudomonas aeruginosa* and c) *Mycobacterium smegmatis*. d) Antibacterial effect of Ag-Cu hybrids in a concentration of 1000 ppm against *M. smegmatis* after a 16h incubation e) Antibacterial effect of Ag-Cu hybrids in a concentration of 200 ppm against *K. pneumoniae* after a 4h incubation. Graph shows the average of three different assays in CFU/mL. Error bars correspond to standard deviation.

In summary, these results indicate that the addition of large amounts of silver in the hybrids do not generate hybrids with better antibacterial properties. This is probably due to the formation of larger silver phosphate species which avoid a proper interaction with the bacterial membrane. However, a big reduction of silver amount in the new hybrids produces nearly imperceptible enhancements over the original hybrid, as seen in Ag_{1.5}Cu₃₅@CALB and Ag₁Cu₃₅@CALB hybrids.

Thus, the hybrids with the most effective antibacterial properties were found when silver amounts between 10% and 3% were incorporated into Cu₃₆@CALB, with Ag₄Cu₃₂@CALB emerging as the most promising candidate.

Therefore, in terms of the mechanism of action against bacteria, these results showed that the compromise between lower amount of silver content and final very small AgNPs located in the surface of the Cu-Nanoflowers make a stronger nanozyme, where Cu enhances the antibacterial efficacy of Ag NPs by the generation of reactive oxygen species (ROS). The synergistic effect is similar to that showed in other systems, for example, where it was demonstrated that was due to a lower binding of Ag⁺ by proteins of the incubation media in the presence of Cu²⁺.³⁰

Other phenomenon could be that these can also act against bacteria by causing membrane damage due to direct interaction with membrane proteins, interfere with nutrient assimilation, lead to protein dysfunction or even be genotoxic.³¹⁻³² On the other hand, it must be considered that Ag(+), can act by specific mechanisms against bacteria, as some studies have shown.^{33,34} In addition to damaging the bacterial wall, silver ions may inhibit DNA replication by forcing it to remain in a condensed state. Additionally, silver ions may interact with sulphur-containing thiol groups of proteins, which are highly responsible for enzymatic activity. Thus, it can be assumed that the improvement in the antibacterial activity of Ag₄Cu₃₂@CALB over Cu₃₆@CALB is due to both synergistic interactions between Cu and Ag and a specific catalytic effect of Ag against bacteria.

Conclusion

A simple and versatile synthesis method for bimetallic Ag-Cu bionanohybrids has been developed through the generation of silver NPs on a previous-formed Cu hybrid. Also, it has been determined that the amount of silver added is a crucial factor in the formation of the bionanohybrids. Higher concentrations of silver result in hybrids with larger and aggregated

nanoparticles, which leads to lower catalytic and antibacterial efficiencies. Conversely, reduced silver concentrations produce hybrids with smaller, less aggregated, and more available silver nanoparticles, resulting in higher activities. This was reflected in the antibacterial assays against *E. coli*, with high antimicrobial activity (4 Log₁₀ reduction) and where improvements of more than one log of inhibition were observed when comparing one of the hybrids with less silver, Ag₄Cu₃₂@CALB to another with more silver, Ag₁₅Cu₂₁@CALB. However, lower amount of silver from 4% (w/w) in the hybrids resulted in a decreased antibacterial capacity.

Ag-Cu bionanohybrids were also shown to be effective against *K. pneumoniae* and *P. aeruginosa* superbugs, obtaining the best log reductions of 7.8 and 4.3, respectively, both with Ag₄Cu₃₂@CALB. Lower efficiencies were obtained against *M. smegmatis*, due to its gram-positive nature, with a maximum value of 1.8 with Ag₄Cu₃₂@CALB.

Based on the results, it can be seen that the bionanohybrid Ag₄Cu₃₂@CALB is an improvement over Cu₃₆@CALB, since it significantly enhances its antibacterial effect. Thus, it has been demonstrated that adding 0.6 mg of silver per mL of Cu₃₆@CALB, results in a highly effective material against bacteria. These findings offer a very interesting opportunity for the development of a super-material capable of killing bacteria, which can be extended to other viral strains or variants, as well as other pathogens such as viruses or fungi.

Experimental Methods

Materials

Copper (II) sulphate pentahydrate [Cu₂SO₄·5H₂O], hydrogen peroxide (H₂O₂, 33% v/v), sodium hydroxide (NaOH) and sodium dihydrogen phosphate 1-hydrate were obtained from Panreac (Barcelona, Spain). Lipase B from *C. antarctica* (CAL-B) solution was obtained from Novozymes (Copenhagen, Denmark). Silver nitrate, *p*-nitrophenol, *p*-aminophenol and sodium borohydride were purchased from Sigma Aldrich. The bacteria models used were *Escherichia coli* C IJ1862 obtained from Prof. James J. Bull, *Klebsiella pneumoniae* from the Serum Statens

Institute Collection, *Pseudomonas aeruginosa* and *Mycobacterium smegmatis* mc²155 from the ATCC collection.

Characterization and Analysis Techniques.

X-ray diffraction (XRD) patterns were obtained using a Texture Analysis D8 ADVANCE Diffractometer (Bruker, Billerica, MA, USA) with Cu K α radiation. Their analysis was performed using the X'Pert Highscore Plus programs.

TEM investigations were performed using an S/TEM Titan 80-300 microscope equipped with a Cetcor Cs probe corrector and energy dispersion X-ray spectrometer (EDS) for chemical composition analysis. Samples for TEM observation were prepared by dispersing a small amount of the material in ethanol and putting a droplet of the suspension on a microscope nickel grid covered with carbon film and allowed to evaporate the alcohol. Then, samples were dried and purified in a plasma cleaner. TEM (Bright Field BF, Dark Field DF, and Selected Area Diffraction) and STEM modes (BF detector to show the structure and morphology; and High Angle Angular Dark Field (HAADF) detector to reveal chemical contrast (Z-contrast)) were used for imaging. Because the tested material was sensitive to the electron beam, during microscopic observations, the intensity of the electron beam and the exposure time were limited. Inductively coupled plasma-optical emission spectrometry (ICP-OES) was performed using an OPTIMA 2100 DV instrument (PerkinElmer, Waltham, MA). A Biocen 22 R (Orto-Alresa, Ajalvir, Spain) refrigerated centrifuge and a Basic Research Telstar LyoQuest freeze-dryer (Steinfurt, Germany) were used in the synthesis of the hybrids. Spectrophotometric analyses were run on a V-730 spectrophotometer (JASCO, Tokyo, Japan). Chromatographic analyses were run using a HPLC system with a pump PU-4180 (JASCO, Tokyo, Japan) and a UV-4075 UV – vis detector (JASCO, Tokyo, Japan). X-ray photoelectron spectroscopy (XPS) spectra were determined through a SPECS GmbH electronic spectroscopy system with a UHV system

(pressure approx. 10-10 mbar), with a PHOIBOS 150 9MCD energy analyzer, monochromatic X-ray sources. The analysis of the same was carried out using the CasaXPS program.

Synthesis of Cu bionanohybrid

Following the previous reported synthesis protocol for copper bionanohybrids [17], 180 mg of commercial Lipase B from *Candida antarctica* (CAL-B) solution was added to 600 mL of sodium phosphate buffer (0.1 M, pH 7) in a 1 L glass bottle containing a small magnetic bar stirrer. Then, 6 g of $\text{Cu}_2\text{SO}_4 \cdot 5\text{H}_2\text{O}$ (10 mg mL^{-1}) was added to the protein solution and the mixture was incubated for 1 h at room temperature. After this time, a light blue emulsion with a concentration of 5000 ppm of the copper bionanohybrid was obtained. The mixture was centrifuged at 8000 rpm for 8 min; the supernatant was removed and the generated pellet with the hybrid was recollected and resuspended in the same initial volume with distilled water (600 mL, 5000 ppm). The process was repeated twice, obtaining the hybrid called $\text{Cu}_{36}\text{@CALB}$.

Synthesis of Ag-Cu bionanohybrids

To generate the silver-copper bionanohybrids, different amounts of silver nitrate (240, 120, 60, 24, 12, 7.2, 4.8 and 2.4 mg) was added to 20 mL of $\text{Cu}_{36}\text{@CALB}$ hybrid. The mixture was stirred for 24 hours at room temperature. After that, it was centrifuged at 8000 rpm for 8 min. The supernatant was removed, and the pellet was resuspended in 15 mL of distilled water. This process was repeated two times more. Finally, the supernatant was removed, and the pellet was resuspended in 2 mL of distilled water. Each solution was collected in a cryotube, frozen with liquid nitrogen, and lyophilized for 16 h. Eight different bionanohybrids were obtained and they were named according to the copper and silver content obtained by ICP-OES: $\text{Ag}_{32}\text{Cu}_8\text{@CALB}$, $\text{Ag}_{15}\text{Cu}_{21}\text{@CALB}$, $\text{Ag}_8\text{Cu}_{28}\text{@CALB}$, $\text{Ag}_6\text{Cu}_{30}\text{@CALB}$, $\text{Ag}_4\text{Cu}_{32}\text{@CALB}$, $\text{Ag}_2\text{Cu}_{34}\text{@CALB}$, $\text{Ag}_{1.5}\text{Cu}_{35}\text{@CALB}$ and $\text{Ag}_1\text{Cu}_{35}\text{@CALB}$. The color of the hybrids lightened from grey to light blue as the amount of silver nitrate was reduced.

Evaluation of catalytic activity (pNP reaction)

A solution of *p*-nitrophenol (pNP) 1mM or 50 mM was prepared in distilled water. Then, 3 mg or 150 mg (respectively) of NaBH₄ was added to 2 mL of pNP to generate the phenolate ion (bright yellow). After 30 seconds, 1 mg of the bionanohybrid was added under gentle stirring at room temperature with a magnetic bar stirrer. The reaction was monitored in the spectrophotometer by measuring the transformation of pNP to *p*-aminophenol (pAP), in the range from 290 to 600 nm, and taking samples at different times. The samples were centrifuged, and an extract of the supernatant was diluted 1:100 with distilled water and added to plastic cuvettes of 1 cm path length.

Evaluation of catalytic activity (pAP reaction)

A solution of *p*-aminophenol (pAP) 1 mM was prepared in 10 mL of distilled water with H₂O₂ 0.5% (v/v). Then, 3 mg of the bionanohybrid was added to the mixture under gently agitation with a magnetic bar stirrer, at room temperature. Samples were taken at different times and centrifuged. Then, 100 μL of the supernatant was diluted 1:10 (with an elution solvent mixture) and injected in HPLC. The elution solvent was a mixture of water – acetonitrile in an 85:15 ratio. A Kromasil C-8 column (5 μm, 150 mm × 4.6 mm) was used, and the injection volume was 10 μL. The degradation of pAP was followed with an UV – vis detector at 254 nm and a flow rate of 0.7 mL/min.

Antibacterial Assays

The antibacterial activity of the bionanohybrids was tested against *Escherichia coli*, *Klebsiella pneumoniae*, *Pseudomonas aeruginosa* and *Mycobacterium smegmatis*. First, suspensions of

different concentrations of the bionanohybrids (1250 and 4000 ppm) were prepared in ultrapure and sterile water. Then, 50 μL of the well-stirred bionanohybrids suspensions were added to 450 or 1000 μL of a LB broth and a stationary bacterial culture mixture, obtaining final concentrations of 125 ppm and 200 ppm for the bionanohybrids. To obtain the final concentration of 1000 ppm, 1 mg of the solid bionanohybrids were added directly to 1 mL of LB broth and a stationary bacterial culture mixture.

The mixtures were thoroughly vortexed and incubated for 4h at 25 °C and 800 rpm. Each sample and bacterial condition was tested in triplicate. From each triplicate, serial dilutions were performed to facilitate the subsequent counting of isolated colonies. After 4h of incubation, 100 μL of each sample was added to an LB+CaCl₂ Petri dish with glass beads. Plates were incubated at 37 °C for 24h (*E. coli*, *P. aeruginosa* and *K. pneumoniae*) and 72h (*M. smegmatis*) and then isolated colonies were counted. The concentration (CFU/mL) of each replicate was calculated for each condition following the Equation 1 and considering the colony count at the optimal dilution and the plated volume. After that, the weighted average was calculated. A negative control (LB) and a positive control (LB with bacteria) are also included in the assay.

$$\frac{CFU}{mL} = \frac{n^{\circ} \text{ colonies}}{\text{volumen of culture plated (mL)}} \times 10^{\text{dilution}} \quad (1)$$

Conflict of Interest

The authors declare no conflict of interest.

Acknowledgements

This work was supported by the Spanish National Research Council (CSIC) (CSIC PTI-Global Health SGL2103036 (J.M.P) and project PIE 202480E088). Authors thank Dr. Martinez from Novozymes. P.D-C. was financially supported by a Ramón y Cajal contract RYC2019-028015-

I funded by MCIN/AEI. We acknowledge support of the publication fee by the CSIC Open Access Publication Support Initiative through its Unit of Information Resources for Research (URICI).

References

1. C. Kim, M. Holm, I. Frost, M. Hasso-Agopsowicz and K. Abbas, Global and Regional Burden of Attributable and Associated Bacterial Antimicrobial Resistance Avertable by Vaccination: Modelling Study *BMJ Glob Health* 2023, **8**, e011341.
2. C.J.L. Murray, K.S. Ikuta, F. Sharara, L. Swetschinski, G. Robles Aguilar, A. Gray, C. Han, C. Bisignano, P. Rao, E. Wool et al, Global Burden of Bacterial Antimicrobial Resistance in 2019: A Systematic Analysis. *The Lancet* 2022, **399**, 629–655.
3. C. Ortega-Nieto, N. Losada-Garcia, D. Prodan, G. Furtos and J.M. Palomo, Recent Advances on the Design and Applications of Antimicrobial Nanomaterials. *Nanomaterials* 2023, **13**, 2406.
4. P.J. Weldick, A. Wang, A.F. Halbus and V.N. Paunov, Emerging Nanotechnologies for Targeting Antimicrobial Resistance. *Nanoscale* 2022, **14**, 4018–4041.
5. D.A. Salazar-Alemán and R.J. Turner, *Microbial Metabolism of Metals and Metalloids*, Springer, Cham **2022**; pp. 77–106.
6. E. Sánchez-López, D. Gomes, G. Esteruelas, L. Bonilla, A.L. Lopez-Machado, R. Galindo, A. Cano, M. Espina, M. Ettcheto, A. Camins, A.M. Silva, A.D. Durazzo, A. Santini, M.L. Garcia and E.B. Souto, Metal-Based Nanoparticles as Antimicrobial Agents: An Overview. *Nanomaterials* 2020, **10**, 292.
7. C. Ortega-Nieto, N. Losada-Garcia, B.C. Pessela, P. Domingo-Calap and J.M. Palomo, Design and Synthesis of Copper Nanobiomaterials with Antimicrobial Properties. *ACS Bio & Med Chem Au* 2023, **3**, 349–358.

8. A. Balestri, J. Cardellini and D. Berti, Gold and Silver Nanoparticles as Tools to Combat Multidrug-Resistant Pathogens. *Curr. Opin. Colloid. Interface Sci.* 2023, **101710**.
9. Y.-J. Kim, Y.-E. Choe, S.-J. Shin, J.-H. Park, K. Dashnyam, H.S. Kim, S.-K. Jun, J.C. Knowles, H.-W. Kim, J.-H. Lee and H.-H. Lee, Photocatalytic Effect-Assisted Antimicrobial Activities of Acrylic Resin Incorporating Zinc Oxide Nanoflakes, *Biomater. Adv.* 2022, **139**, 213025.
10. A. Pormohammad and R.J. Turner, Silver Antibacterial Synergism Activities with Eight Other Metal(Loid)-Based Antimicrobials against Escherichia Coli, Pseudomonas Aeruginosa, and Staphylococcus Aureus, *Antibiotics* 2020, **9**, 853.
11. T.L. Meister, J. Fortmann, M. Breisch, C. Sengstock, E. Steinmann, M. Köller, S. Pfaender and A. Ludwig, *Sci. Rep.* 2022, **12**, 7193.
12. O. T. Fanoro and O. S. Oluwafemi, Bactericidal antibacterial mechanism of plant synthesized silver, gold and bimetallic nanoparticles. *Pharmaceutics* 2020, **12**, 1044.
13. Z. Hao, M. Wang, L. Cheng, M. Si, Z. Feng and Z Feng, Synergistic antibacterial mechanism of silver-copper bimetallic nanoparticles. *Front. Bioeng. Biotechnol.* 2024, **11**, 1337543.
14. J.M. Palomo, A New Concept for Metal Nanoparticles Synthesis. *Chem. Commun.* 2019, **55**, 9583–9589.
15. N. Losada-Garcia, A. Jimenez-Alesanco, A.Velazquez-Campoy, O. Abian and J.M. Palomo, Enzyme/Nanocopper Hybrid Nanozymes: Modulating Enzyme-like Activity by the Protein Structure for Biosensing and Tumor Catalytic Therapy, *ACS Appl. Mat. Int.* 2021, **13**, 5111-5124.
16. R. Benavente, D. Lopez-Tejedor, M.P. Morales, C. Perez-Rizquez, J.M. Palomo, The enzyme-induced formation of iron hybrid nanostructures with different morphologies. *Nanoscale* 2020, **12**, 12917-12927.

17. N. Losada-Garcia, A. Vazquez-Calvo, D. Ortega-Alarcon, O. Abian, A. Velazquez-Campoy, P. Domingo-Calap, A. Alcami and J.M. Palomo, Nanostructured Biohybrid Material with Wide-Ranging Antiviral Action. *Nano Res.* 2023, **16**, 11455–11463.
18. N. Losada-Garcia, A. Vazquez-Calvo, A. Alcami and J.M. Palomo, Preparation of Highly Stable and Cost-Efficient Antiviral Materials for Reducing Infections and Avoiding the Transmission of Viruses Such as SARS-CoV-2, *ACS Appl. Mater. Interfaces* 2023, **15**, 22580–22589.
19. N. Losada-Garcia, A. Rodriguez-Otero and J.M. Palomo, Fast Degradation of Bisphenol A in Water by Nanostructured CuNPs@CALB Biohybrid Catalysts. *Nanomaterials* 2019, **10**, 7.
20. N. Losada-García, A. Rodríguez-Otero and J.M. Palomo, Tailorable Synthesis of Heterogeneous Enzyme–Copper Nanobiohybrids and Their Application in the Selective Oxidation of Benzene to Phenol. *Catal. Sci. Technol.* 2020, **10**, 196–206.
21. A. Ahmed, M. Usman, Z. Ji, M. Rafiq, B. Yu, Y. Shen and H. Cong, Nature-Inspired Biogenic Synthesis of Silver Nanoparticles for Antibacterial Applications. *Mater Today Chem* 2023, **27**, 101339.
22. J.M. Naapuri, N. Losada-Garcia, J. Deska and J.M. Palomo, Synthesis of Silver and Gold Nanoparticles–Enzyme–Polymer Conjugate Hybrids as Dual-Activity Catalysts for Chemoenzymatic Cascade Reactions. *Nanoscale* 2022, **14**, 5701–5715.
23. X. Sui, X. Wang, H. Huang, G. Peng, S. Wang, Z. Fan, A novel photocatalytic material for removing microcystin-LR under visible light irradiation: degradation characteristics and mechanisms , *PLoS One* 2014, **22**, 9.
24. P. Liu, P. Ferrer-Borrell, M. Božič, V. Kokol, K. Oksman and A.P. Mathew, Nanocelluloses and their phosphorylated derivatives for selective adsorption of Ag(+), Cu(2+) and Fe(3+) from industrial effluents, *J. Hazard. Mat.* 2015, **294**, 177-185.

25. N. Kircheva, S. Angelova, S. Dobrev, V. Petkova, V. Nikolova and T. Dudev, Cu⁺/Ag⁺ Competition in Type I Copper Proteins (T1Cu), *Biomolecules* 2023, **13**, 681.
26. X. Fan, L. Yahia and E. Sacher, Antimicrobial Properties of the Ag, Cu Nanoparticle System.. *Biology* 2021, **10**, 137.
27. U. F. Gunpath, H. Le, R. D. Handy and C. Tredwin, Anodised TiO₂ nanotubes as a scaffold for antibacterial silver nanoparticles on titanium implants. *Mater. Sci. Eng. C* 2018, **91**, 638–644.
28. A. M. El Badawy, R. G. Silva, B. Morris, K. G. Scheckel, M. T. Suidan and T. M. Tolaymat, Surface Charge-Dependent Toxicity of Silver Nanoparticles. *Environ. Sci. Technol.* 2011, **45**, 283–287.
29. Structures. In *Medical Microbiology*. University of Texas Medical Branch at Galveston: Galveston (TX), 1996 ISBN 0963117211.
30. G. Vasiliev, A.-L. Kubo, H. Vija, A.Kahru, D. Bondar, Y.Karpichev and O. Bondarenko, Synergistic antibacterial effect of copper and silver nanoparticles and their mechanism of action. *Sci.Rep.* 2023, *13*, Article number: 9202.
31. M. Godoy-Gallardo, U. Eckhard, L.M. Delgado, Y.J.D. de Roo Puente, M. Hoyos-Nogués, F.J. Gil and R.A. Perez, Antibacterial Approaches in Tissue Engineering Using Metal Ions and Nanoparticles: From Mechanisms to Applications. *Bioact. Mater.* 2021, **6**, 4470–4490.
32. J.A. Lemire, J.J. Harrison and R.J.Turner, Antimicrobial Activity of Metals: Mechanisms, Molecular Targets and Applications. *Nat. Rev. Microbiol.* 2013, **11**, 371–384.
33. Q.L. Feng, J. Wu, G.Q. Chen, F.Z. Cui, T.N. Kim and J.O. Kim. A Mechanistic Study of the Antibacterial Effect of Silver Ions on Escherichia Coli and Staphylococcus Aureus. *J Biomed. Mater. Res.* 2000, **52**, 662–668.

34. I. Matai, A. Sachdev, P. Dubey, S. Uday Kumar, B. Bhushan and P. Gopinath, Antibacterial Activity and Mechanism of Ag–ZnO Nanocomposite on *S. Aureus* and GFP-Expressing Antibiotic Resistant *E. Coli*. *Colloids Surf. B* 2014, **115**, 359–367.